THE JOURNAL OF PHYSICAL CHEMISTRY Letters

pubs.acs.org/JPCL Letter

Transition from Doublet to Triplet Excitons in Single Perovskite Nanocrystals

Chunyang Yin,[#] Yan Lv,[#] Xiangtong Zhang, Yu Zhang, William W. Yu, Chunfeng Zhang, Zhi-Gang Yu, Xiaoyong Wang,* and Min Xiao*

Cite This: J. Phys. Chem. Lett. 2020, 11, 5750−5755 Read Online

ACCESS | Metrics & More | Article Recommendations | Supporting Information

ABSTRACT: Lead halide perovskite nanocrystals (NCs) have emerged as novel semiconductor nanostructures possessing great potential for optoelectronic, photovoltaic, and quantum information processing applications. Success in these applications requires a comprehensive understanding of the perovskite NCs' electronic structures, which mysteriously exhibit either doublet or triplet peaks of exciton luminescence at the single-particle level. Here we show that the transition from doublet- to triplet-exciton peaks can be triggered in single $CsPbI_3$ NCs from the same batch of samples when they are stored in the ambient environment. We propose theoretically that the doublet-exciton peaks originate from two in-plane dipole moments, while the optical transition arising from the out-of-plane dipole moment becomes prominent only after the crystal-field splitting is strongly reduced by the structural transformation in the deterioration process. Furthermore, the quantum-confinement effect is strongly reinforced in the single $CsPbI_3$ NCs with a triplet-exciton configuration, leading to enhanced Auger recombination and allowing us to extract the emission-energy dependence of the exciton-energy-level fine structure.

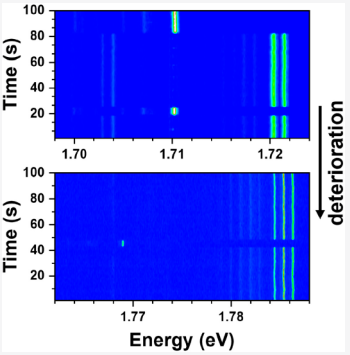

Since the discovery of single-photon emission in single lead halide perovskite nanocrystals (NCs),[1] a variety of superior optical properties have been reported for these novel semiconductor nanostructures, including a large absorption cross section,[2] blinking-free photoluminescence (PL),[3] and bright-exciton fine structure splitting (FSS) resolved at cryogenic temperatures.[4−9] The exact energy-level alignments of lead halide perovskite NCs are still being vigorously debated, as is the origin of the bright-exciton FSS, which is manifested as either doublet or triplet PL peaks at the single-particle level. On one hand, the doublet and triplet PL peaks are believed to arise from the intrinsic bright-exciton sublevels of tetragonal and orthorhombic crystal phases, respectively, mediated by the crystal field and the electron−hole exchange interaction (EI).[5,6,9,10] On the other hand, the Rashba effect might be triggered in lead halide perovskite NCs due to the existence of a lattice or surface imperfection that breaks the inversion symmetry,[7] which could place the dark-exciton singlet state higher in energy than the bright-exciton triplet ones,[8] as argued in detail by Sercel et al. in a theoretical work.[11] In a recent magneto-optical study, however, Tamarat et al. show that the lowest exciton state in single $FAPbBr_3$ (FA = formamidinium) NCs is dark.[12] It is obvious that both the electron−hole EI and Rashba effect are intimately related to the structural parameters, which could potentially serve as potent knobs for tuning the exciton recombination patterns of single lead halide perovskite NCs for a full understanding of their underlying electronic structures.

Here we show that the size of perovskite $CsPbI_3$ NCs can be naturally reduced in the ambient environment to cause a blue shift in their ensemble PL peak. Interestingly, the doublet and triplet PL peaks are predominantly observed in single $CsPbI_3$ NCs from the fresh and transformed samples, respectively. For single $CsPbI_3$ NCs with triplet PL peaks, the charged excitons are associated with a low fluorescent efficiency and the optical emission of neutral biexcitons is completely missing, presumably caused by nonradiative Auger recombination. Moreover, their FSS values of neutral single excitons are significantly larger than those of single $CsPbI_3$ NCs with doublet PL peaks. While the findings presented above signify an enhancement of the quantum-confinement effect, we propose that it is the accompanying structural transformation from orthorhombic to "cubiclike" phases that triggers the transition from doublet to triplet excitons. The doublet PL peaks of a single $CsPbI_3$ NC should originate from two bright states with in-plane dipole moments, while the other with an out-of-plane dipole moment acquires a significant oscillator strength only after this structural transformation.

The perovskite $CsPbI_3$ NCs used in this experiment were chemically synthesized according to an established procedure[13] with slight modifications[3,6] (see the experimental details in the Supporting Information). As reported previously,[14] the $CsPbI_3$

Received: June 22, 2020
Accepted: June 26, 2020
Published: June 26, 2020

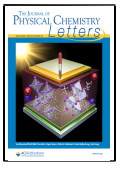

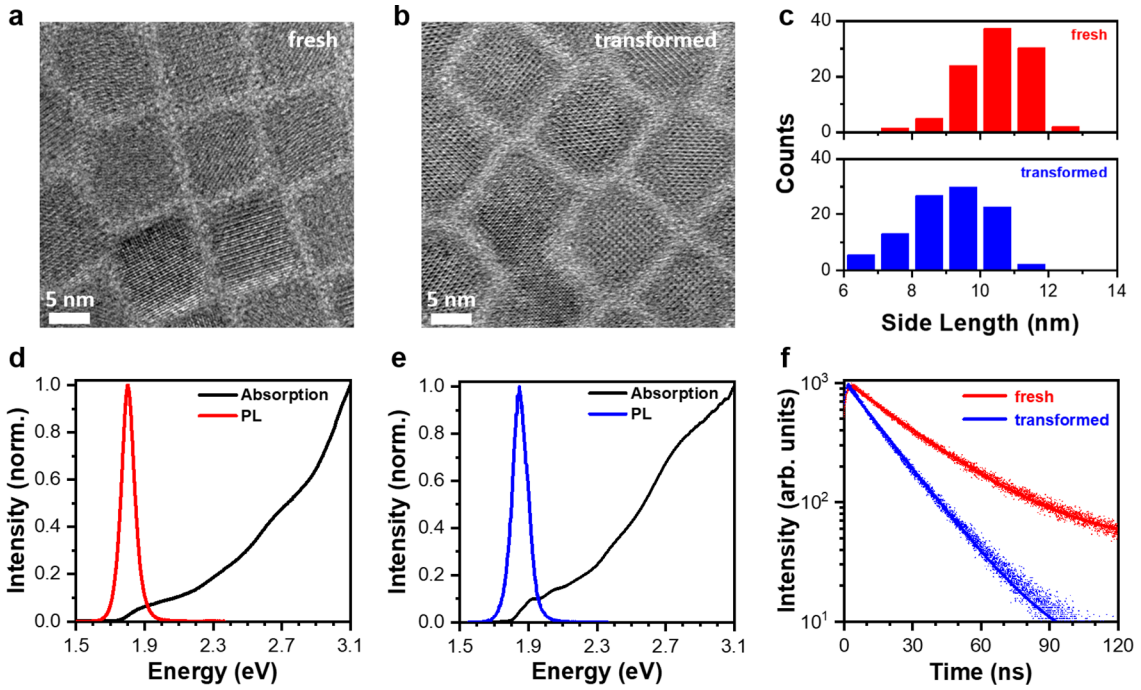

Figure 1. Structural and optical characterizations of ensemble $CsPbI_3$ NCs at room temperature. Transmission electron microscope images for the (a) fresh and (b) transformed $CsPbI_3$ NCs. (c) Statistical histograms for the size distributions of the fresh (top) and transformed (bottom) $CsPbI_3$ NCs. Solution emission and absorption spectra measured for the (d) fresh and (e) transformed $CsPbI_3$ NCs. (f) PL decay curves measured for the fresh and transformed $CsPbI_3$ NCs with single-exponential lifetime fittings of ∼29.4 and ∼17.6 ns, respectively.

NCs contained in a polar solvent and exposed to the ambient environment would suffer from a fast decomposition process to cause a layer-by-layer exfoliation of the constituent materials. In our case where the $CsPbI_3$ NCs had been stored in a weak polar solvent of toluene for approximately two months, their average size was reduced from the initial size of 10.4 ± 0.9 nm to the final size of 9.0 ± 1.1 nm as estimated from the transmission electron microscopy measurements (see Figure 1a−c and Figure S1). Accompanying this size reduction, the room-temperature PL peak measured in solution for ensemble $CsPbI_3$ NCs was blue-shifted from ∼690 to ∼670 nm, while the featureless band-edge absorption evolved into a discernible peak located at ∼646 nm (see Figure 1d,e). Meanwhile, the ensemble PL lifetime decreased significantly from the initial value of ∼29.4 ns measured for the fresh sample to a value of ∼17.6 ns for the transformed one (see Figure 1f). This shortened PL lifetime suggests the possible introduction of nonradiative exciton decay channels in the $CsPbI_3$ NCs during the deterioration process (see the experimental details in the Supporting Information).

For the optical studies of single $CsPbI_3$ NCs at the cryogenic temperature of 4 K (see Figure S2 and experimental details in the Supporting Information), a 570 nm picosecond fiber laser operated at 5.6 MHz was used with the output power being set at $\langle N \rangle$ = 0.1 unless otherwise specified in the text, where $\langle N \rangle$ corresponds to the average number of excitons created per pulse in a single $CsPbI_3$ NC.[2,3,6,15] An energy range of ∼1.70−1.77 eV was covered by the optical emission of single $CsPbI_3$ NCs from the fresh sample, with ∼15% of them possessing a single PL peak with a line width close to our spectral resolution of ∼200 μeV and only ∼5% having a PL triplet (see Figure S3). Meanwhile, ∼80% of the studied single $CsPbI_3$ NCs emitted a PL doublet with orthogonally and linearly polarized peaks (see Figure 2a). It has been well established in cesium lead halide NCs that the energy-level structure of band-edge excitons is composed of three bright states in addition to a dark one.[5,7,8] If two of the bright states are degenerate in a tetragonal crystal structure, a PL doublet would be observed in a single $CsPbI_3$ NC with one peak being linearly polarized and the other unpolarized or circularly polarized.[5,9] This possibility can be safely ruled out because each of the doublet PL peaks emitted from a single $CsPbI_3$ NC showed an almost complete linear polarization (see Figure 2a). For all of the doublet PL peaks resolved from single $CsPbI_3$ NCs, an average FSS value of ∼350 μeV could be obtained, which is close to the thermal energy of k_BT = 348 μeV at 4 K, with k_B being the Boltzmann constant. It is then unlikely that the highest-energy one of the three bright states is not thermally populated,[8] because its exciton occupation probability is still ∼13.5% with respect to the lowest-energy one, as estimated from the Maxwell−Boltzmann distribution[16] with an energy separation of 700 μeV.

After we had switched to the transformed sample, it was surprising to see that ∼90% of the single $CsPbI_3$ NCs emitted triplet PL peaks covering the energy range of ∼1.74−1.84 eV. As shown in Figure 2b and also revealed in several recent reports,[5,8,9] each of the triplet PL peaks possesses a linear-polarization behavior. In Figure S4, we have further provided detailed PL intensity mappings as a function of the polarization angle for the triplet PL peaks from several additional single $CsPbI_3$ NCs. When we increased the laser power to set $\langle N \rangle$ = 1.0, it was easy to observe optical emission of neutral biexcitons from all of the single $CsPbI_3$ NCs studied in the fresh sample with doublet PL peaks (see Figure 2c and Figure S5a). In stark contrast, optical emission from neutral biexcitons was completely missing in nearly all of the single $CsPbI_3$ NCs studied in the transformed sample with triplet PL peaks (see Figure 2d and Figure S5b), implying that nonradiative Auger

https://dx.doi.org/10.1021/acs.jpclett.0c01939
J. Phys. Chem. Lett. 2020, 11, 5750−5755

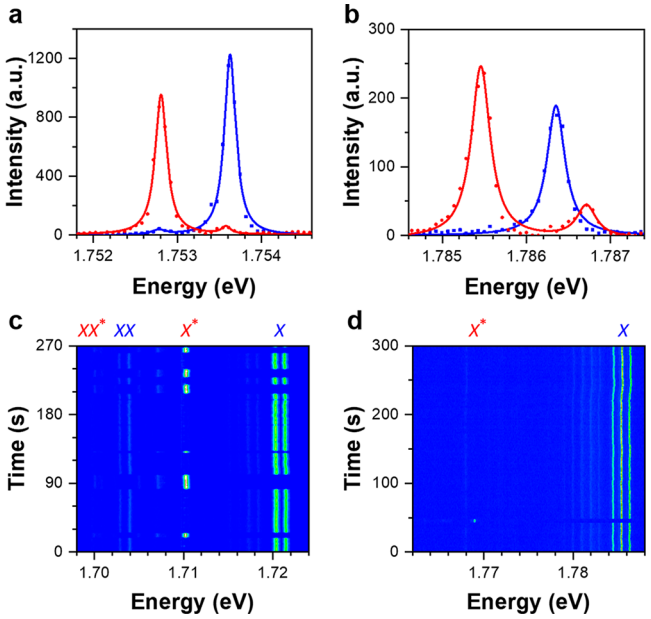

Figure 2. PL spectral measurements of single $CsPbI_3$ NCs at 4 K. PL spectra measured for a representative single $CsPbI_3$ NC from (a) the fresh sample and (b) the transformed sample at polarization angles of 0° (red) and 90° (blue), respectively. In panels a and b, the single $CsPbI_3$ NCs were excited at $\langle N \rangle$ = 0.1 with an unpolarized laser beam, while the value of 0° corresponded to the detection polarization angle at which a maximum PL intensity was obtained for the lowest-energy PL peak. Time-dependent PL spectral image measured at $\langle N \rangle$ = 1.0 for a representative single $CsPbI_3$ NC from (c) the fresh sample and (d) the transformed sample, with unpolarized laser excitation and PL detection. Here *X*, *X**, *XX*, and *XX** denote neutral single excitons, charged single excitons, neutral biexcitons, and charged biexcitons, respectively. Each of the PL spectra shown in panels a–d was acquired with an integration time of 1 s.

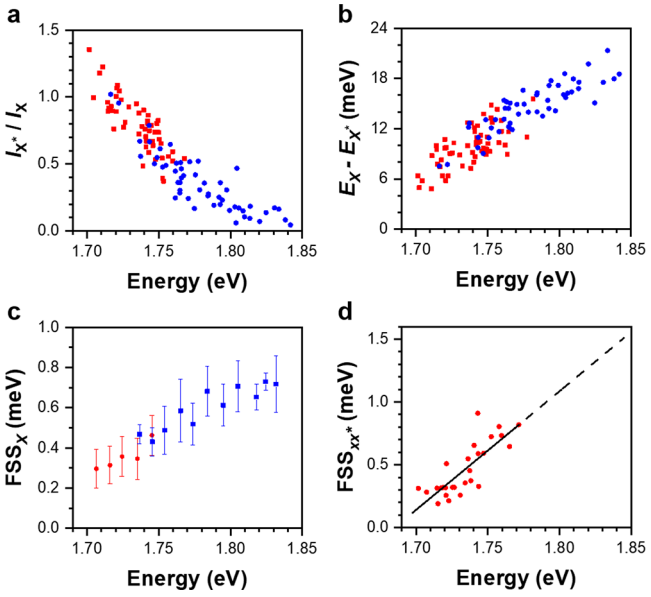

Figure 3. Emission-energy-dependent optical properties of single $CsPbI_3$ NCs. (a) PL intensity ratio between charged and neutral single excitons plotted as a function of emission energy for 52 and 54 single $CsPbI_3$ NCs from the fresh sample (red) and the transformed sample (blue), respectively. (b) Binding energy of charged single excitons plotted as a function of emission energy for 58 and 51 single $CsPbI_3$ NCs from the fresh sample (red) and the transformed sample (blue), respectively. The binding energy is calculated as the emission-energy difference between the neutral and charged single excitons of a single $CsPbI_3$ NC. (c) FSS value of neutral single excitons plotted as a function of emission energy for 89 and 113 single $CsPbI_3$ NCs from the fresh sample (red) and the transformed sample (blue), respectively. The emission energies of different single $CsPbI_3$ NCs are binned at an interval of 10 meV, while the error bar at each emission energy reflects the distribution range of FSS values around the central average data point. (d) FSS value of charged biexcitons plotted as a function of emission energy for 26 single $CsPbI_3$ NCs from the fresh sample. The data points in the low-energy range are linearly fitted with a solid line that is extended to the high-energy range with a dashed line to guide the eye.

recombination of multiple excitons is strongly enhanced in these small $CsPbI_3$ NCs.[17,18] As shown in Figure 2c and Figure S5a, optical emission of charged single excitons and charged biexcitons can also be resolved in the single $CsPbI_3$ NCs from the fresh sample with doublet PL peaks, while only charged single-exciton emission exists in the single $CsPbI_3$ NCs from the transformed sample with triplet PL peaks (see Figure 2d and Figure S5b). The origins of various PL peaks mentioned above, such as from charged single excitons, neutral biexcitons, and charged biexcitons, were discussed in detail in a previous report focusing on the exciton FSSs of single $CsPbI_3$ NCs.[6]

For each of the single $CsPbI_3$ NCs studied in our experiment from the fresh (transformed) sample with a PL doublet (triplet), we could calculate the PL intensity ratio between the charged and neutral single excitons, which is plotted with a red (blue) data point in Figure 3a as a function of emission energy (hereafter defined as the average energy of doublet or triplet PL peaks). Because the small $CsPbI_3$ NCs are more vulnerable to nonradiative Auger recombination,[17] this PL intensity ratio decreases almost linearly with an increase in emission energy. This enhanced Auger recombination is also reflected in the PL lifetime ratio between the charged and neutral single excitons, decreasing from an average value of ~0.6 for single $CsPbI_3$ NCs in the fresh sample to ~0.3 for those in the transformed sample (see panels c and d of Figure S5 for representative PL decay curves). Furthermore, the binding energy of charged single excitons increases almost linearly with an increase in emission energy (see Figure 3b), which suggests that the electron–hole attraction is more enhanced for charged single excitons in the small $CsPbI_3$ NCs. On the basis of the decreasing PL efficiency/lifetime and the increasing binding energy of charged single excitons, as well as the missing emission of neutral biexcitons, we can conclude that the quantum confinement is indeed reinforced in single $CsPbI_3$ NCs from the transformed sample.

Because the same ligands were covering the surfaces of the single $CsPbI_3$ NCs in the fresh and transformed samples, their possible contribution to the transition from doublet to triplet excitons could be excluded. In a previous report employing the effective-mass and electron–hole EI theories,[11] the size dependence of the exciton fine structures was calculated for perovskite $CsPbBr_3$ NCs from the weak to the strong quantum-confinement regimes. It was discovered that the energy-level orders and especially the oscillator strengths of bright-exciton states were not affected by the quantum-confinement effect. In our experiment, we have synthesized many batches of $CsPbI_3$ NCs with different sizes and, consequently, slightly different ensemble PL peaks. Without the ambient deterioration process, a majority of these single $CsPbI_3$ NCs would still emit doublet PL peaks. On the basis of

https://dx.doi.org/10.1021/acs.jpclett.0c01939
J. Phys. Chem. Lett. 2020, 11, 5750–5755

the discussions mentioned above, we can infer that, instead of size reduction and ligand change,[19,20] there must exist another origin for the transition from doublet to triplet excitons observed here in single $CsPbI_3$ NCs.

The energy-level structure of band-edge excitons in $CsPbI_3$ NCs is composed of two in-plane orthogonal states (X and Y), one out-of-plane state (Z), and one dark state (D).[5,8,9] These exciton states and the associated oscillator strengths can be reliably described by the effective-mass model developed recently for hybrid organic–inorganic lead halides[21] (see detailed discussions in the Supporting Information). The band gap energy and exciton binding energy of the fresh $CsPbI_3$ NCs are similar to those of their bulk counterpart, which has been shown to possess an orthorhombic crystal structure.[22] On the basis of the calculated band edges and effective masses from recent first-principles calculations,[21] we can obtain a crystal-field splitting of −0.65 eV between the $6P_x$ and $6P_z$ orbitals, together with the anisotropic Kane parameters ($P_{\parallel}$ = 5.81 eV/Å, and $P_{\perp}$ = 7.12 eV/Å). More importantly, the conduction band is formed predominantly by the $6P_x$ and $6P_y$ orbitals (total weight of ∼0.855) with only a small portion of the $6P_z$ orbital (weight of ∼0.145).

For the $CsPbI_3$ NCs from the transformed sample, the size reduction effect in the deterioration process could make them more "cubiclike" in the crystal structure,[23] yielding a smaller crystal-field splitting as reflected in the absorption spectrum typical for the perovskite materials with zero-dimensional quantum confinement[24] (Figure 1e). As shown in Figure S6, the calculated ratio between the Z and X oscillator strengths is significantly enhanced when the crystal-field splitting is reduced, leading to the eventual emergence of an additional PL peak from the activated Z excitons. In addition to the reinforced quantum confinement induced by size reduction, this structural change from orthorhombic to "cubiclike" phases may also contribute to the enhanced Auger recombination of charged single excitons and neutral biexcitons in the single $CsPbI_3$ NCs from the transformed sample. We note, however, it is still challenging to precisely determine whether the cesium lead halide NCs are associated with a cubic[13] or orthorhombic[25] crystal structure. As revealed from the synchrotron X-ray diffraction measurements on perovskite $CsPbCl_3$ NCs,[26] the conversions between cubic and orthorhombic crystal phases are strongly dependent on the existence of structural defects, which could be introduced into the $CsPbI_3$ NCs studied here during the deterioration process.

After proposing that a phase transition is triggered in the transformed $CsPbI_3$ NCs, we now move on to discuss how the size reduction and the reinforced quantum confinement affect the exciton FSS values in terms of the variation of the emission energy. Here we assume that the "cubiclike" crystal structure is manifested mainly by a reduced crystal field, while the exciton fine structures are still dictated by the orthorhombic phase in a transformed $CsPbI_3$ NC. For the PL triplet, we can define $(\Delta E_1 + \Delta E_2)/2$ as the FSS value for neutral single excitons, where ΔE_1 (ΔE_2) is the energy separation between the two nearby PL peaks with the high (medium) and medium (low) energies. As shown in Figure 3c, the FSS value of a single $CsPbI_3$ NC with either a PL doublet from the fresh sample (red data point) or a PL triplet from the transformed sample (blue data point) shows increases with emission energy, which is similarly manifested in the ΔE_1 and ΔE_2 values (see Figure S7a). For the single $CsPbI_3$ NCs from the fresh sample with a PL doublet, the FSS value of charged biexcitons with a PL doublet is plotted in Figure 3d to show also a positive correlation with the emission energy. The FSS values at higher emission energies are missing in Figure 3d, because no optical emission was observed from the charged biexcitons in small $CsPbI_3$ NCs.

For low-dimensional semiconductor nanostructures, the isotropic and anisotropic electron–hole EIs are proportional to the FSS values of charged biexcitons and neutral single excitons, respectively.[27,28] Ignoring more complex theoretical models,[29,30] we have simply adopted linear fittings for the emission-energy dependencies of the FSS values obtained from neutral single excitons (see Figure S7a) and charged biexcitons (see Figure 3d), the results of which are jointly plotted in Figure S7b. It can be seen that the charged-biexciton FSS value gradually exceeds that of the neutral single excitons with an increase in emission energy, which we believe could also be related to the transition from doublet to triplet excitons. Notably in a previous report on ensemble CdTe/CdS NCs,[31] where the isotropic electron–hole EI between the trapped hole in the Cd vacancy and the conduction-band electron on the surface approached the FSS value of the neutral single excitons, the transition from doublet to triplet excitons would also occur to demonstrate possibly a common feature of this interesting electronic phenomenon.

In colloidal CdSe NCs, the anisotropic electron–hole EI has been estimated to be 2.5 times larger than the isotropic electron–hole EI.[30] Similarly in our case of $CsPbI_3$ NCs, the anisotropic electron–hole EI is no longer treated as a perturbation term. Using the FSS values obtained from neutral single excitons (see Figure S7a) and charged biexcitons (see Figure 3d), we depict in Figure 4a the emission-energy

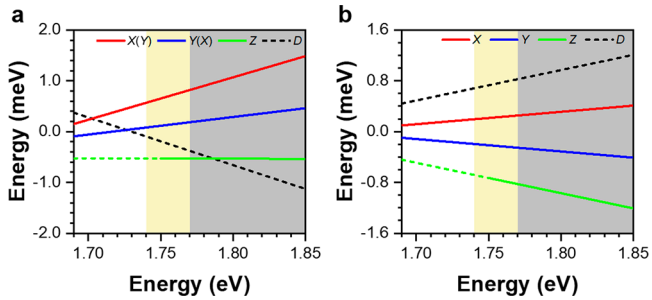

Figure 4. Exciton-energy-level structures of single $CsPbI_3$ NCs. Emission-energy dependence of the exciton-energy-level structure within (a) the electron–hole EI model and (b) the Rashba model. In panels a and b, the energy-level structure is composed of three bright-exciton states (X, Y, and Z) and one dark-exciton state (D). A dashed line is always drawn for the non-emissive D state but partially for the Z state at the low emission-energy range where its optical emission was not observed in the experiment. The level order of the bright X and Y states can be determined in the Rashba model shown in panel b but not in the electron–hole EI model shown in panel a, so that $X(Y)$ and $Y(X)$ are used to specify this uncertain situation.

dependencies of the X, Y, Z, and D energy positions in reference to their average value set at the energy of zero, where the bright-exciton Z state is assumed to have an energy lower than those of the X and Y states (see detailed discussions in the Supporting Information).[5,9,11] As one can see in Figure 4a, the energy positions and separations of the bright-exciton X, Y, and Z states continue to increase with emission energy. Meanwhile, the dark-exciton D state is lying above the bright-exciton states at lower emission energies, deviating from what is predicted

https://dx.doi.org/10.1021/acs.jpclett.0c01939
J. Phys. Chem. Lett. 2020, 11, 5750−5755

from the electron−hole EI theory that it should always be the lowest-energy ground exciton state.[5,9,10,12] This strongly suggests that some other factors, such as the anisotropic shape and the Rashba effect,[8,11,32] need to be included in future theoretical works for a full description of the exciton electronic structures.

While the exciton-energy-level structures presented in Figure 4a are based on the electron−hole EI, we have additionally considered how they would evolve with the emission energy under the sole influence of the Rashba effect. Using the same Hamiltonian as in ref 8 with the triplet peak energies obtained experimentally from single $CsPbI_3$ NCs in the transformed sample (see Figure S8), we plot in Figure 4b the emission-energy dependencies of the *X*, *Y*, *Z*, and *D* energy levels (see detailed discussions in the Supporting Information). In this Rashba scenario originally depicted by Becker et al. to set the *D* state at the highest-energy position,[8] the energy separation measured here between any two neighboring states increases with emission energy. This may imply possible enhancement of the Rashba effect due to the decrease in size, which takes effect by increasing the surface-to-volume ratio and electron−phonon coupling[7,8,33,34] (see Figure S9).

To summarize, we have proposed that a phase transition is triggered in the size reduction process of perovskite $CsPbI_3$ NCs upon deterioration in the ambient environment. When combined with the theoretical results based on an effective-mass model, our experimental data suggest that one of the three bright-exciton states with an out-of-plane dipole moment is only weakly emissive for the fresh orthorhombic $CsPbI_3$ NCs. This weak out-of-plane dipole moment is significantly enhanced in the transformed "cubiclike" $CsPbI_3$ NCs with a reduced crystal field. The findings presented above have thus solved a long-standing puzzle in the optical studies of single perovskite NCs, where doublet PL peaks are sometimes observed with orthogonal and linear polarizations. On the basis of the FSS values obtained for both neutral single excitons and charged biexcitons, we can describe phenomenologically how the exciton-energy-level structures of a single $CsPbI_3$ NC evolve in the two scenarios of the electron−hole EI and Rashba effect. In reality, these two mechanisms could work together to determine the exact exciton-energy-level structures, even inducing crossovers between the bright- and dark-exciton states at specific sizes of the $CsPbI_3$ NCs.

■ ASSOCIATED CONTENT

Supporting Information

The Supporting Information is available free of charge at https://pubs.acs.org/doi/10.1021/acs.jpclett.0c01939.

Experimental details, theoretical calculations, transmission electron microscopy images, optical setup for the single-NC PL measurements, PL spectra of a single $CsPbI_3$ NC from the fresh sample with triplet peaks, variations of intensity with the polarizer angles for the triplet PL peaks of single $CsPbI_3$ NCs from the transformed sample, PL spectra measured at high laser powers for single $CsPbI_3$ NCs with doublet and triplet peaks, PL decay curves measured for neutral and charged single excitons, ratio of oscillator strengths calculated as a function of the crystal-field splitting, emission-energy dependencies of the neutral-exciton and charged-biexciton FSSs, energy positions of the triplet PL peaks obtained for single $CsPbI_3$ NCs from the transformed sample, PL spectra measured for single $CsPbI_3$ NCs with LO phonon replicas, and intensity ratios measured between the LO phonon replica and the neutral-exciton peak as a function of emission energy (PDF)

■ AUTHOR INFORMATION

Corresponding Authors

Xiaoyong Wang − *National Laboratory of Solid State Microstructures, School of Physics, and Collaborative Innovation Center of Advanced Microstructures, Nanjing University, Nanjing 210093, China;* orcid.org/0000-0003-1147-0051; Email: wxiaoyong@nju.edu.cn

Min Xiao − *National Laboratory of Solid State Microstructures, School of Physics, and Collaborative Innovation Center of Advanced Microstructures, Nanjing University, Nanjing 210093, China; Department of Physics, University of Arkansas, Fayetteville, Arkansas 72701, United States*; Email: mxiao@uark.edu

Authors

Chunyang Yin − *National Laboratory of Solid State Microstructures, School of Physics, and Collaborative Innovation Center of Advanced Microstructures, Nanjing University, Nanjing 210093, China*

Yan Lv − *National Laboratory of Solid State Microstructures, School of Physics, and Collaborative Innovation Center of Advanced Microstructures, Nanjing University, Nanjing 210093, China*

Xiangtong Zhang − *State Key Laboratory of Integrated Optoelectronics and College of Electronic Science and Engineering, Jilin University, Changchun 130012, China*

Yu Zhang − *State Key Laboratory of Integrated Optoelectronics and College of Electronic Science and Engineering, Jilin University, Changchun 130012, China;* orcid.org/0000-0003-2100-621X

William W. Yu − *State Key Laboratory of Integrated Optoelectronics and College of Electronic Science and Engineering, Jilin University, Changchun 130012, China;* orcid.org/0000-0001-5354-6718

Chunfeng Zhang − *National Laboratory of Solid State Microstructures, School of Physics, and Collaborative Innovation Center of Advanced Microstructures, Nanjing University, Nanjing 210093, China;* orcid.org/0000-0001-9030-5606

Zhi-Gang Yu − *ISP/Applied Sciences Laboratory and Department of Physics and Astronomy, Washington State University, Spokane, Washington 99210, United States;* orcid.org/0000-0002-1376-9025

Complete contact information is available at: https://pubs.acs.org/10.1021/acs.jpclett.0c01939

Author Contributions

#C.Y. and Y.L. contributed equally to this work.

Notes

The authors declare no competing financial interest.

■ ACKNOWLEDGMENTS

This work is supported by the National Basic Research Program of China (2019YFA0308704 and 2017YFA0303700), the National Natural Science Foundation of China (61974058, 11574147, and 11621091), and the PAPD of Jiangsu Higher Education Institutions.

REFERENCES

(1) Park, Y.-S.; Guo, S.; Makarov, N. S.; Klimov, V. I. Room temperature single-photon emission from individual perovskite quantum dots. *ACS Nano* **2015**, *9*, 10386−10393.

(2) Hu, F.; Zhang, H.; Sun, C.; Yin, C.; Lv, B.; Zhang, C.; Yu, W. W.; Wang, X.; Zhang, Y.; Xiao, M. Superior optical properties of perovskite nanocrystals as single photon emitters. *ACS Nano* **2015**, *9*, 12410−12416.

(3) Hu, F.; Yin, C.; Zhang, H.; Sun, C.; Yu, W. W.; Zhang, C.; Wang, X.; Zhang, Y.; Xiao, M. Slow Auger recombination of charged excitons in nonblinking perovskite nanocrystals without spectral diffusion. *Nano Lett.* **2016**, *16*, 6425−6430.

(4) Rainò, G.; Nedelcu, G.; Protesescu, L.; Bodnarchuk, M. I.; Kovalenko, M. V.; Mahrt, R. F.; Stöferle, T. Single cesium lead halide perovskite nanocrystals at low temperature: fast single-photon emission, reduced blinking, and exciton fine structure. *ACS Nano* **2016**, *10*, 2485−2490.

(5) Fu, M.; Tamarat, P.; Huang, H.; Even, J.; Rogach, A. L.; Lounis, B. Neutral and charged exciton fine structure in single lead halide perovskite nanocrystals revealed by magneto-optical spectroscopy. *Nano Lett.* **2017**, *17*, 2895−2901.

(6) Yin, C.; Chen, L.; Song, N.; Lv, Y.; Hu, F.; Sun, C.; Yu, W. W.; Zhang, C.; Wang, X.; Zhang, Y.; Xiao, M. Bright-exciton fine-structure splittings in single perovskite nanocrystals. *Phys. Rev. Lett.* **2017**, *119*, 026401.

(7) Isarov, M.; Tan, L. Z.; Bodnarchuk, M. I.; Kovalenko, M. V.; Rappe, A. M.; Lifshitz, E. Rashba effect in a single colloidal $CsPbBr_3$ perovskite nanocrystal detected by magneto-optical measurements. *Nano Lett.* **2017**, *17*, 5020−5026.

(8) Becker, M. A.; Vaxenburg, R.; Nedelcu, G.; Sercel, P. C.; Shabaev, A.; Mehl, M. J.; Michopoulos, J. G.; Lambrakos, S. G.; Bernstein, N.; Lyons, J. L.; Stoferle, T.; Mahrt, R. F.; Kovalenko, M. V.; Norris, D. J.; Raino, G.; Efros, A. L. Bright triplet excitons in caesium lead halide perovskites. *Nature* **2018**, *553*, 189−193.

(9) Ramade, J.; Andriambariarijaona, L. M.; Steinmetz, V.; Goubet, N.; Legrand, L.; Barisien, T.; Bernardot, F.; Testelin, C.; Lhuillier, E.; Bramati, A.; Chamarro, M. Fine structure of excitons and electron-hole exchange energy in polymorphic $CsPbBr_3$ single nanocrystals. *Nanoscale* **2018**, *10*, 6393−6401.

(10) Nestoklon, M. O.; Goupalov, S. V.; Dzhioev, R. I.; Ken, O. S.; Korenev, V. L.; Kusrayev, Y. G.; Sapega, V. F.; de Weerd, C.; Gomez, L.; Gregorkiewicz, T.; Lin, J.; Suenaga, K.; Fujiwara, Y.; Matyushkin, L. B.; Yassievich, I. N. Optical orientation and alignment of excitons in ensembles of inorganic perovskite nanocrystals. *Phys. Rev. B: Condens. Matter Mater. Phys.* **2018**, *97*, 235304.

(11) Sercel, P. C.; Lyons, J. L.; Wickramaratne, D.; Vaxenburg, R.; Bernstein, N.; Efros, A. L. Exciton fine structure in perovskite nanocrystals. *Nano Lett.* **2019**, *19*, 4068−4077.

(12) Tamarat, P.; Bodnarchuk, M. I.; Trebbia, J.-B.; Erni, R.; Kovalenko, M. V.; Even, J.; Lounis, B. The ground exciton state of formamidinium lead bromide perovskite nanocrystals is a singlet dark state. *Nat. Mater.* **2019**, *18*, 717−724.

(13) Protesescu, L.; Yakunin, S.; Bodnarchuk, M. I.; Krieg, F.; Caputo, R.; Hendon, C. H.; Yang, R. X.; Walsh, A.; Kovalenko, M. V. Nanocrystals of cesium lead halide perovskites ($CsPbX_3$, X = Cl, Br, and I): novel optoelectronic materials showing bright emission with wide color gamut. *Nano Lett.* **2015**, *15*, 3692−3696.

(14) Yuan, G.; Ritchie, C.; Ritter, M.; Murphy, S.; Gómez, D. E.; Mulvaney, P. The degradation and blinking of single $CsPbI_3$ perovskite quantum dots. *J. Phys. Chem. C* **2018**, *122*, 13407−13415.

(15) Makarov, N. S.; Guo, S.; Isaienko, O.; Liu, W.; Robel, I.; Klimov, V. I. Spectral and dynamical properties of single excitons, biexcitons, and trions in cesium-lead-halide perovskite quantum dots. *Nano Lett.* **2016**, *16*, 2349−2362.

(16) Shen, Q.; Ripolles, T. S.; Even, J.; Ogomi, Y.; Nishinaka, K.; Izuishi, T.; Nakazawa, N.; Zhang, Y.; Ding, C.; Liu, F.; Toyoda, T.; Yoshino, K.; Minemoto, T.; Katayama, K.; Hayase, S. Slow hot carrier cooling in cesium lead iodide perovskites. *Appl. Phys. Lett.* **2017**, *111*, 153903.

(17) Li, Y.; Wu, K. Size and halide dependent Auger recombination in lead halide perovskite nanocrystals. *Angew. Chem., Int. Ed.* **2020**, DOI: 10.1002/anie.202004668.

(18) Klimov, V. I.; Mikhailovsky, A. A.; McBranch, D. W.; Leatherdale, C. A.; Bawendi, M. G. Quantization of multiparticle Auger rates in semiconductor quantum dots. *Science* **2000**, *287*, 1011−1013.

(19) Liu, L.; Zhao, R.; Xiao, C.; Zhang, F.; Pevere, F.; Shi, K.; Huang, H.; Zhong, H.; Sychugov, I. Size-dependent phase transition in perovskite nanocrystals. *J. Phys. Chem. Lett.* **2019**, *10*, 5451−5457.

(20) Sarang, S.; Bonabi Naghadeh, S.; Luo, B.; Kumar, P.; Betady, E.; Tung, V.; Scheibner, M.; Zhang, J. Z.; Ghosh, S. Stabilization of the cubic crystalline phase in organometal halide perovskite quantum dots via surface energy manipulation. *J. Phys. Chem. Lett.* **2017**, *8*, 5378−5384.

(21) Yu, Z. G. Effective-mass model and magneto-optical properties in hybrid perovskites. *Sci. Rep.* **2016**, *6*, 28576.

(22) Sutton, R. J.; Filip, M. R.; Haghighirad, A. A.; Sakai, N.; Wenger, B.; Giustino, F.; Snaith, H. J. Cubic or orthorhombic? Revealing the crystal structure of metastable black-phase $CsPbI_3$ by theory and experiment. *ACS Energy Lett.* **2018**, *3*, 1787−1794.

(23) Swarnkar, A.; Marshall, A. R.; Sanehira, E. M.; Chernomordik, B. D.; Moore, D. T.; Christians, J. A.; Chakrabarti, T.; Luther, J. M. Quantum dot-induced phase stabilization of alpha-$CsPbI_3$ perovskite for high-efficiency photovoltaics. *Science* **2016**, *354*, 92−95.

(24) Hirasawa, M.; Ishihara, T.; Goto, T. Exciton features in 0-, 2-, and 3-dimensional networks of $[PbI_6]^{4-}$ octahedral. *J. Phys. Soc. Jpn.* **1994**, *63*, 3870−3879.

(25) Bertolotti, F.; Protesescu, L.; Kovalenko, M. V.; Yakunin, S.; Cervellino, A.; Billinge, S. J. L.; Terban, M. W.; Pedersen, J. S.; Masciocchi, N.; Guagliardi, A. Coherent nanotwins and dynamic disorder in cesium lead halide perovskite nanocrystals. *ACS Nano* **2017**, *11*, 3819−3831.

(26) Ma, J.-P.; Yin, J.; Chen, Y.-M.; Zhao, Q.; Zhou, Y.; Li, H.; Kuroiwa, Y.; Moriyoshi, C.; Li, Z.-Y.; Bakr, O. M.; Mohammed, O. F.; Sun, H.-T. Defect-triggered phase transition in cesium lead halide perovskite nanocrystals. *ACS Mater. Lett.* **2019**, *1*, 185−191.

(27) Akimov, I. A.; Hundt, A.; Flissikowski, T.; Henneberger, F. Fine structure of the trion triplet state in a single self-assembled semiconductor quantum dot. *Appl. Phys. Lett.* **2002**, *81*, 4730−4732.

(28) Akimov, I. A.; Kavokin, K. V.; Hundt, A.; Henneberger, F. Electron-hole exchange interaction in a negatively charged quantum dot. *Phys. Rev. B: Condens. Matter Mater. Phys.* **2005**, *71*, 075326.

(29) Efros, A. L.; Rosen, M. The electronic structure of semiconductor nanocrystals. *Annu. Rev. Mater. Sci.* **2000**, *30*, 475−521.

(30) Sercel, P. C.; Efros, A. L. Band-edge exciton in CdSe and other II−VI and III−V compound semiconductor nanocrystals - revisited. *Nano Lett.* **2018**, *18*, 4061−4068.

(31) Lifshitz, E.; Fradkin, L.; Glozman, A.; Langof, L. Optically detected magnetic resonance studies of colloidal semiconductor nanocrystals. *Annu. Rev. Phys. Chem.* **2004**, *55*, 509−557.

(32) Sercel, P. C.; Lyons, J. L.; Bernstein, N.; Efros, A. L. Quasicubic model for metal halide perovskite nanocrystals. *J. Chem. Phys.* **2019**, *151*, 234106.

(33) Yaffe, O.; Guo, Y.; Tan, L. Z.; Egger, D. A.; Hull, T.; Stoumpos, C. C.; Zheng, F.; Heinz, T. F.; Kronik, L.; Kanatzidis, M. G.; Owen, J. S.; Rappe, A. M.; Pimenta, M. A.; Brus, L. E. Local polar fluctuations in lead halide perovskite crystals. *Phys. Rev. Lett.* **2017**, *118*, 136001.

(34) Fu, M.; Tamarat, P.; Trebbia, J.-B.; Bodnarchuk, M. I.; Kovalenko, M. V.; Even, J.; Lounis, B. Unraveling exciton-phonon coupling in individual $FAPbI_3$ nanocrystals emitting near-infrared single photons. *Nat. Commun.* **2018**, *9*, 3318.

https://dx.doi.org/10.1021/acs.jpclett.0c01939
J. Phys. Chem. Lett. 2020, 11, 5750−5755